

ON THE EFFECT OF WIND ON THE OPTICAL – MICROPHYSICAL CHARACTERISTICS OF COASTAL MARINE HAZE

V.V. Veretennikov

*Institute of Atmospheric Optics
Siberian Branch of the Academy of Sciences of the USSR, Tomsk
Received January 8, 1990*

A method and some results of an interpretation of the spectral aerosol extinction coefficients of the atmosphere over a coastal marine region aimed at retrieving the quantitative information on the microstructure of a haze and its transformation caused by the wind velocity are presented. The effect of wind velocity on the relative content of the submicron and coarsely dispersed fractions is analyzed based on the solution of the inverse problem and the angular dependences of the aerosol scattering phase functions in the visible and IR are reconstructed for different wind velocities. The results obtained can be used in solving the problems of taking into account the transformation of the optical–microphysical properties of the haze under the effect of wind.

Introduction. This paper is the continuation of the previous studies of the microphysical structure of atmospheric hazes performed in Refs. 1–3 under different geophysical conditions based on interpretation of their light scattering characteristics by the inverse–problem method. To determine the general behavior of the variability of the haze microphysical parameters caused by the effect of the aerosol formation and transformation mechanisms under various geographic and meteorological conditions, we used for the initial data the optical models of the polarization scattering phase functions¹ and the spectral extinction² of the coastal marine haze as well as the model of the scattering matrix components of continental haze.³ The extinction coefficient at $\lambda = 0.55 \mu\text{m}$ was also chosen for the input parameter of the models since its variability is to a great extent caused by the simultaneous effect of a number of processes of aerosol formation and transformation.

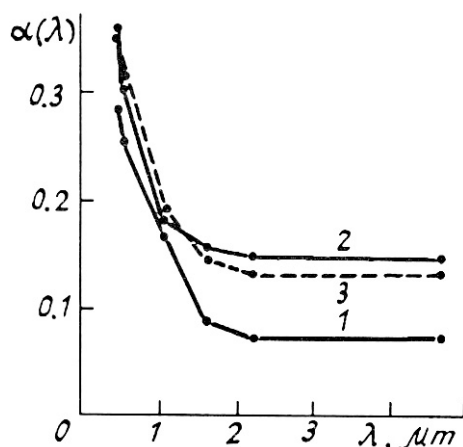


FIG. 1. The average spectral dependence of the aerosol extinction coefficients $\alpha(\lambda)$ for the ranges of wind velocity: [0.6–2.1] (curve 1), [2.2–3.7] (curve 2), and [3.8–5.8] m/s (curve 3) in the layer of the atmosphere adjacent to water over a coastal marine region.⁴

To study the effect of any individual geophysical factor on the optical–physical characteristics of the haze we must chose the experimental data obtained under the conditions

when other external factors remain unchanged. This noticeably reduces the bulk of experimental data available for the analysis. An example of the solution of such a problem is given in Ref. 4 where the effect of wind velocity on the aerosol extinction in the visible and IR in the coastal marine atmosphere is studied. The data analyzed in Ref. 4 were obtained on the basis of statistical processing of the measurement data on the spectral transmission of the atmosphere over the Crimea coast of the Black Sea (Tarkhankut peninsula) under steady sea winds. The path traverses the bay at an altitude of 4 m above the sea level. Under these conditions a data file comprising 32 experimental realizations divided into subfiles according to the ranges of the wind velocity [0.6–52.1], [2.2–53.7], and [3.8–55.8] m/s was taken for an analysis. Relative humidity of air for the data file under study varied from 72 to 96%, with the mean values for each subfile being about 82%.

The wind velocity near the sea surface along with the air humidity are the main factors affecting the salt aerosol microstructure. Analysis of the results of experimental investigations^{5,6} of the marine aerosol inflow into the atmosphere with increase of the wind velocity indicate not only the monotonic increase of the salt aerosol mass concentration but also the transformation of the dispersion composition due to the increase of the coarsely dispersed fraction of particles. An attempt to describe this dependence quantitatively give ambiguous results⁵ depending on specific geophysical factors of a concrete region.

The statistical analysis of experimental data performed in Ref. 4 indicated that the increase of the wind velocity up to 3 m/s is accompanied by an increase in the aerosol extinction coefficients $\alpha(\lambda)$ (Fig. 1) for the entire wavelength range under study. This agrees fairly well with the direct microstructural measurements^{5,6} and with the data of numerical simulations.⁷ However, with further increase of the wind velocity up to 6 m/s the aerosol extinction coefficients in the IR decrease. This nonmonotonic dependence of $\alpha(\lambda)$ on the wind velocity is physically interpreted in Ref. 4. Based on the inverse–problem solution we determine the dispersed structure of aerosol haze which, by the spectral behavior of the light extinction, is adequate to the wind velocity dependence obtained in Ref. 4. In addition, we estimated the effect of wind velocity on the relative content of the submicron and coarsely dispersed fractions of particles.

2. The method for solving the inverse problem. In constructing the algorithm of inverting the spectral dependence of the aerosol extinction coefficient it was assumed *a priori* that the unknown microstructural distribution of aerosol is formed by the submicron (s) ($r < 1 \mu\text{m}$) and coarsely dispersed (c) fractions. This assumption is favored by interpretation of a single-parameter model of the spectral light extinction of the coastal marine haze² as well as by the data on the spectral dependence of the light extinction coefficients obtained by Pkhalagov and Uzhegov⁸ based on the linear multiple regressive analysis. In accordance with the above discussion, we can represent the aerosol extinction coefficient $\alpha(\lambda)$ in the form

$$\alpha(\lambda) = \alpha_s(\lambda) + \alpha_c(\lambda) = \int_0^R K(\lambda, r)[s_s(r) + s_c(r)]dr, \quad (1)$$

where $K(\lambda, r)$ is the extinction efficiency factor of a spherical particle of radius r , $s(r)$ is the distribution of particles over size of geometric cross section, and the subscripts "s" and "c" denote the submicron and coarsely dispersed fractions, respectively. It is well known that spectral measurements of the aerosol extinction coefficient contain large amount of information on the content of the particles with size close in value to the wavelength λ . The developed algorithm accounts for the difference in the optical manifestations of the two aerosol fractions caused by the spectral characteristics of the extinction efficiency factor $K(\lambda, r)$ in different spectral ranges. In the visual range the factor $K(\lambda, r)$ for the "c" fraction is close to the constant and weakly oscillates with decreasing amplitude about 2, so that the extinction coefficient may be taken to be equal to $\alpha_c(\lambda) \approx 2S_c$, where S_c is the total geometric cross section of the "c" aerosol fraction. Equation (1) for visual range is written in the form

$$\int_0^{r^*} K(\lambda, r)s_s(r)dr + 2S_c = \alpha(\lambda), \quad (2)$$

where $r^* = 1 \mu\text{m}$ is the boundary value of the particle size between the "s" and "c" fractions. It can be seen from Eq. (2) the existence of the "c" fraction shifts the spectral characteristics $\alpha(\lambda)$ at the quantity $2S_c$. It should be noted, however, that measurements of $\alpha(\lambda)$ do not contain enough information on the "c" fraction of the distribution $s(r)$, and bear the information only on its total content – total cross section S_c . Therefore, Eq. (2) is determined for the size distribution $S_s(r)$ of the "s" fraction and can be solved using the well-known regularizing algorithms.⁹ In this case S_c can be considered as one of the unknown values.

Conversely, measurements of $\alpha(\lambda)$ in the IR bear the information primarily on the content of the "c" fraction of particles while the contribution of the "s" fraction to the extinction of IR radiation is negligible and is determined by the behavior of the kernel $K(\lambda, r) \sim \lambda^{-c}$, where "c" is the constant. Thus Eq. (1) takes the form

$$\int_0^R K(\lambda, r)s_c(r) + A\lambda^{-c} = \alpha(\lambda), \quad (3)$$

where $s_c(r)$ is the unknown distribution of the "c" aerosol fraction, and the second term in the left side represents the

contribution of the "s" aerosol fraction to the light extinction in the IR.

The scheme of simultaneous inversion of system of Eqs. (2) and (3) for the unknown functions $s_s(r)$ and $s_c(r)$ can formally be described as follows. Let us consider a discrete analog of Eq. (1)

$$Ks = \alpha \quad (4)$$

and represent a vector of the sought solution in the form of the direct sum $s = s_s \oplus s_c$. Then system of equations (2) and (3) can be written in the form

$$\begin{aligned} A_1 s_s + A_2 s_c &= \alpha_1, \\ A_3 s_s + A_4 s_c &= \alpha_2, \end{aligned} \quad (5)$$

where $A_1, A_2, A_3,$ and A_4 are the matrices forming the matrix

$$K = \begin{pmatrix} A_1 & A_2 \\ A_3 & A_4 \end{pmatrix} \quad (6)$$

and the vectors α_1 and α_2 form the direct sum $\alpha = \alpha_1 \oplus \alpha_2$. Let the vector s_s be determined from the first equation of system (5) and s_c – from the second equation. As a result, we can write

$$s_s = A_1^+(\alpha_1 - A_2 s_c); \quad s_c = A_4^+(\alpha_2 - A_3 s_s), \quad (7)$$

where A_1^+ and A_4^+ are the pseudoinverse matrices to the matrices A_1 and A_4 . To find the unknown vectors s_s and s_c from Eqs. (7) the iteration method can be used. In the simplest case the iterative process is constructed as follows.

For the initial approximation $s_c^{(0)}$ the solution $s_s^{(1)}$ of the first equation of system (7) is found and subsequently substituted into the right side of the second equation of system (7), from which the solution $s_c^{(1)}$ is found. The iterations are then repeated. A sufficient condition of iteration convergence has the form

$$\frac{\|A_2\| \|A_3\|}{\|A_1\| \|A_4\|} \leq q < 1.$$

Taking into account the structure of Eq. (2) the initial approximation $A_2 s_c^{(0)}$ in the right side of Eq. (7) can be replaced by the value $2S_c^{(0)}$.

Thus, in the given scheme of reconstructing the microstructural distribution $s(r)$ based on its decomposition into the "s" and "c" fractions, inverting system (4) of large dimensionality was replaced by the successive inverting two systems (7) of smaller dimensionality. The efficiency of this method was tested in numerical experiments. In practice this procedure leads to increased stability and accuracy of the inverse-problem solution. A regularizing algorithm similar to that used in Ref. 2 with the choice of the regularization parameter according to the rule of minimum discrepancies¹⁰ was employed in numerical realization of the described method of constructing the approximate solutions s_s and s_c by inverting Eqs. (7). The reconstructed solution

$s^{(+)} = Ps$ (P is the projection operator onto a set of nonnegative functions) was then additionally multiplied by the parameter

$$\gamma = \frac{(As^{(+)}, \alpha)}{(As^{(+)}, As^{(+)})}$$

ensuring the minimum to the discrepancy functional $\rho^2 = \|\gamma APs - \alpha\|^2$.

3. The results of inversion. The spectral dependences of real $m(\lambda)$ and imaginary $\kappa(\lambda)$ parts of the complex refractive index needed for calculation of the kernel $K(\lambda, r)$ were chosen consistent with the meteorological visibility range S_m — the input parameter of the optical-meteorological model of the haze¹ — in the same way as in Ref. 2. The spectral dependences of the aerosol extinction coefficient $\alpha(\lambda)$ chosen for inverting are shown in Fig. 1 and correspond to the mean wind velocities 1.4, 3.0, and 4.7 m/s (curves 1–3) for the meteorological visibility range varying from 12 to 15 km.

The results of inversion of the experimental data presented in Fig. 1 are shown in Figs. 2a and b. The analysis of these results show that the type of the reconstructed microstructural distributions is similar to the haze model described in Ref. 2. The common feature for all reconstructed distributions $s(r)$ is, as expected *a priori*, the distinct manifestation of the two fractions with the boundary near 0.8–1.0 μm . The amplitude of the submicron fraction of the distribution (Fig. 2a) having unimodal structure significantly exceeds (by 1–2 orders of magnitude) the amplitude of the coarsely dispersed fraction. The available spectral information does not allow us to reconstruct the "c" fraction with high particle size resolution. This fraction of the size distribution is shown in Fig. 2b in the interval 1–55 μm in the form of a histogram with the 1 μm step size.

The existence of the two ranges of the particle size in the reconstructed distributions $s(r)$ is caused by two different mechanisms of marine aerosol formation as a result of collapse of air bubbles at the sea surface¹¹. The relative contributions of the "s" and "c" aerosol fractions to the extinction of visible and IR radiation agree fairly well with the *a priori* assumptions. In fact, as the results of inversion show, even for minimum wind velocity and consequently for minimum influence of the wind regime on carrying out the salt particles in the atmosphere, the contribution of the "s" aerosol fraction to the extinction coefficient $\alpha(\lambda)$ in the near-IR does not exceed 29% and decreases to 2.8% with increase of the wavelength up to 4.66 μm , so that the extinction of radiation in this wavelength range is determined primarily by the "c" aerosol fraction. In spite of the fact that the contribution of the particles of "c" aerosol fraction to the total geometric cross section is relatively small (20–36%, see Fig. 3a), these particles make also a significant contribution to the extinction of visible radiation. They contribute 32% of the total extinction in the left end of the spectral interval and their contribution increases to 62% at $\lambda = 1.06 \mu\text{m}$ ($v = 3 \text{ m/s}$). However, the absolute contribution of the "c" fraction of particles to the light extinction in the wavelength region 0.48–1.06 μm is approximately constant and for the last example it is equal to 0.112 km^{-1} . Therefore, the shape of the spectral curve $\alpha(\lambda)$ in the indicated wavelength region is independent of the "c" fraction and is determined by the "s" particles.

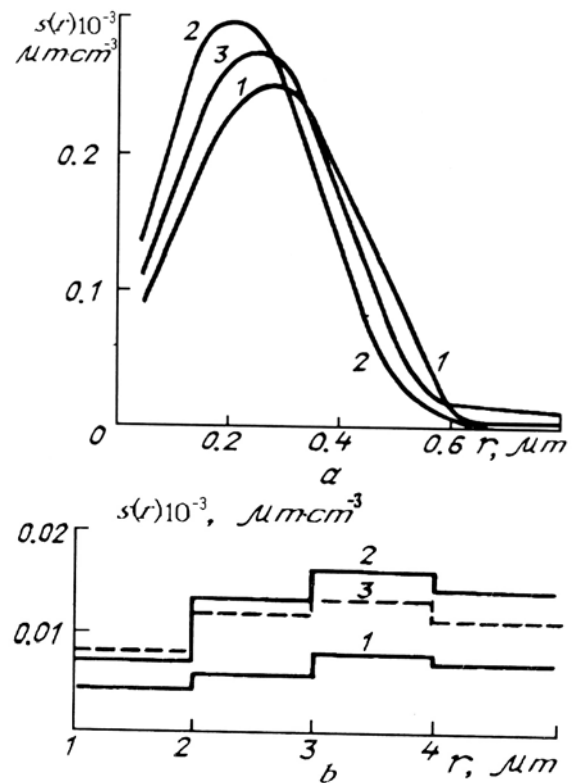


FIG. 2. The variability of the microstructure of the haze caused by the wind obtained using the results of inversion of the experimental data shown in Fig. 1 1) $v = 1.4 \text{ m/s}$, 2) $v = 3.0 \text{ m/s}$, and 3) $v = 4.7 \text{ m/s}$; a) submicron fraction; b) coarsely dispersed fraction.

As follows from the data presented in Refs. 5–7, the concentration of the particles, in particular large ones, monotonically increases with increase of the wind velocity. The results of our study show that the wind velocity affects the "c" aerosol fraction to a greater extent. Thus, if the total geometric cross section S increases insignificantly from 0.12 to 0.15 km^{-1} with increase of the wind velocity from 1.4 to 4.7 m/s, then the relative contribution of the "c" aerosol fraction varies from 20 to 36% ($v = 3.0 \text{ m/s}$) decreasing to 32.5% for $v = 4.7 \text{ m/s}$ (Fig. 3a). At the same time, the cross section of "s" fraction remains within narrow limits 0.097–0.1 km^{-1} .

Thus, the results of inversion indicate the nonmonotonic character of variations in the total cross section of the particles S versus wind velocity v . This is primarily caused by the "c" aerosol fraction, which finally leads to the nonmonotonic dependence of the spectral aerosol extinction coefficients in the IR on the wind velocity.

The indicated relation between the microstructural parameters of the haze and the wind velocity in the boundary layer of the atmosphere adjacent to water becomes more pronounced for the distribution function of particles over their volumes. When the wind velocity varies from 1.4 to 3.0 m/s, the volume fill factor increases by a factor of 1.8 from $1.42 \cdot 10^{-10}$ to $2.5 \cdot 10^{-10}$ and then decreases to $2.3 \cdot 10^{-10}$ for $v = 4.7 \text{ m/s}$ (Fig. 3b). In contrast to the geometric cross section S , the largest part of the volume of

particles (and hence of their mass) in this case constitute the particles of the "c" fraction (73.5–87.6%), which play a dominant role in the dependence of particle mass concentration on the wind velocity. For comparison, the dashed line in Fig. 3b shows the dependence of volume content of aerosol particles which was calculated from the experimental data given in Ref. 5 for mass concentration of chlorides measured for different sea wind velocities (station Katsiveli). In calculations the fraction of sea salts in the total mass of the coastal aerosol was taken from the experimental data given in Ref. 5 for the particle density of 2.2 g/cm^3 . The agreement of the data obtained by interpreting the optical measurements with the results of processing of the impact or samples taken in the coastal region of the Black Sea can be considered to be satisfactory taking into account a wide range of variations in the dependences of the content of the salt particles on the wind velocity observed in the experiments over other seas. ^{5,6}

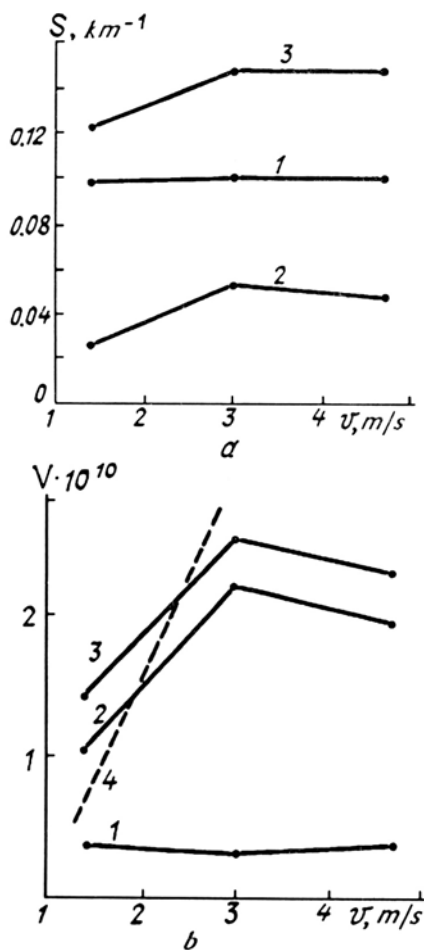


FIG. 3. Dependence of the particle geometric cross sections S (a) and the volume file factor V (b) on the wind velocity: 1) submicron fraction, 2) coarsely dispersed fraction, 3) their total magnitude, and 4) results of the calculations from the experimental data given in Ref. 5.

Finally it should be noted that the "c" fraction of aerosol, which plays a decisive role in nonmonotonic dependence of $\alpha(\lambda)$ on the wind velocity, constitutes not more than 1% of the total number of aerosol particles. Their number density is about one particle per cubic centimeter for the wind

velocity $v = 1.4 \text{ m/s}$ and increases by a factor of 2.5 with increase of v up to 4.7 m/s .

4. **Retrieval of scattering phase functions.** Variations of the microphysical parameters of the haze under the effect of wind velocity influence not only the variability of the spectral extinction but also the angular light-scattering characteristics which can be determined from the reconstructed aerosol microstructure. As an example, Fig. 4 shows the scattering phase functions $\mu(\theta)$ calculated from the microstructural data shown in Fig. 2 for the two values of wind velocity $v = 1.4 \text{ m/s}$ (curves 1 and 3) and 3.0 m/s (curves 2 and 4). The scattering phase functions 1 and 2 have been reconstructed at the radiation wavelength $\lambda = 0.55$ while 3 and 4 at $\lambda = 4.66 \mu\text{m}$. The scattering phase function in the visible spectral range are characterized by a narrow peak at small scattering angles ($\theta \ll 5^\circ$, curves 1 and 2 in Fig. 4b). As can be seen from the results of comparison of the data shown in Fig. 4, the scattering phase functions in the visible range are influenced by the wind velocity within small scattering angles near the forward direction as well as in the back hemisphere. A small-angle part of the scattering phase function (Fig. 4b), where its value is determined by the "c" fraction of aerosol particles, is most sensitive to the variations of the wind velocity. For the remaining scattering angles the variations in the scattering phase functions depends weakly on the wind velocity and within the angles 5 – 150° , do not exceed 13–17%. Going over to the IR, the scattering phase function becomes less elongated and shifts at identical values as the wind velocity increases from 1.4 to 3.0 m/s, corresponding to its increase approximately by a factor of two for the entire scattering angles (curves 3 and 4).

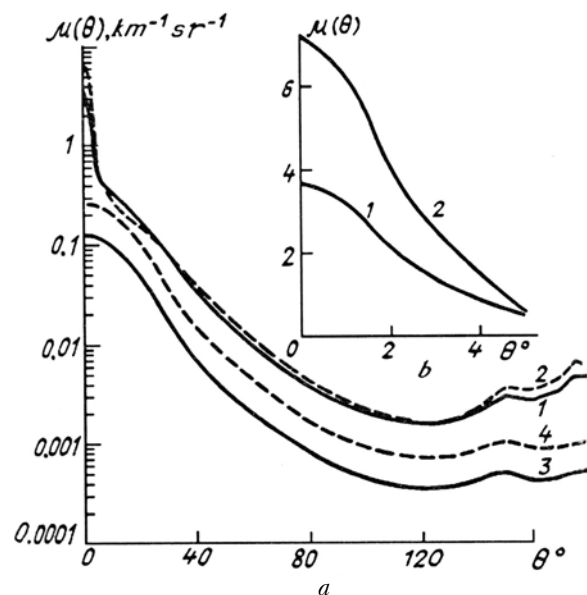


FIG. 4. Scattering phase functions $\mu(\theta)$ calculated from microstructural data shown in Fig. 2 for $v = 1.4 \text{ m/s}$ (curves 1 and 3) and 3.0 m/s (curves 2 and 4); curves 1, 2) $\lambda = 0.55 \mu\text{m}$; curves 3, 4) $\lambda = 4.66 \mu\text{m}$.

5. **Conclusion.** Thus, the quantitative data on the microstructure of the coastal haze over the Black Sea region and transformation of its submicron and coarsely dispersed fractions depending on the wind velocity have been studied using the inverse-problem method for the spectral aerosol extinction coefficients. It is shown that the wind velocity

most strongly affects the content of the coarsely dispersed fraction which is equal to about 74–88% of the total mass of aerosol particles for the conditions of observations. The results obtained verify the hypothesis set up in Ref. 4 on the role of the coarsely dispersed aerosol fraction in nonmonotonic dependence of the aerosol extinction coefficients in the IR on the wind velocity. The angular dependences of the light scattering characteristics retrieved from the microstructural data are indicative of the strong effect of the wind velocity on the variations of the small-angle scattering phase function in the visible range. The results obtained can be used when the variability of the optical–microphysical models of the marine haze under the effect of wind velocity must be taken into account.

REFERENCES

1. V.V. Veretennikov, M.V. Kabanov, and M.V. Panchenko, *Izv. Akad. Nauk SSSR, Ser. FAO* **22**, No. 10, 1042–1049 (1986).
2. V.V. Veretennikov, *Atm. Opt.* **3**, No. 10, 939–946 (1990).
3. G.I. Gorchakov, A.S. Emilenko, and M.A. Sviridenkov, *Izv. Akad. Nauk SSSR, Ser. FAO* **17**, No. 1, 39–49 (1981).
4. Yu.A. Pkhalagov, V.N. Uzhegov, and N.N. Shchelkanov, *Izv. Akad. Nauk SSSR, Ser. FAO* **23**, No. 3, 324–327 (1987).
5. O.P. Petrenchuk, *Experimental Studies of Atmospheric Aerosol* (Gidrometeoizdat, Leningrad, 1979), 264 pp.
6. S. Tsunogai, O. Saito, K. Ymada, and S. Nakaya, *J. Geophys. Res.* **77**, No. 27, 5283–5292 (1972).
7. W.C. Wells, G. Gal, and M.W. Munn, *Appl. Opt.* **16**, No. 3, 654–659 (1977).
8. M.V. Kabanov, M.V. Panchenko, Yu.A. Pkhalagov, et. al., *Optical Properties of Coastal Marine Hazes* (Nauka, Novosibirsk, 1988), 201 pp.
9. V.E. Zuev and I.E. Naats, *Inverse Problems of Laser Sounding of the Atmosphere* (Nauka, Novosibirsk, 1988), 242 pp.
10. V.P. Tanana, *Methods of Solving the Operator Equations* (Nauka, Moscow, 1981), 156 pp.
11. S. Rasul, ed., *Chemistry of the Lower Atmosphere* [Russian translation] (Mir, Moscow, 1976), 408 pp.

